HYDROLOGICAL PROCESSES
Hydrol. Process. **18**, 1975–1997 (2004)
Published online 3 February 2004 in Wiley InterScience (www.interscience.wiley.com). DOI: 10.1002/hyp.1343

Active microwave remote sensing for soil moisture measurement: a field evaluation using ERS-2

Jeffrey P. Walker,[1]* Paul R. Houser[1] and Garry R. Willgoose[2]

[1] *Hydrological Sciences Branch, Laboratory for Hydrospheric Processes, NASA Goddard Space Flight Center, Greenbelt, Maryland 20771, USA*

[2] *Department of Civil, Surveying and Environmental Engineering, The University of Newcastle, Callaghan, New South Wales 2308, Australia*

Abstract:

Active microwave remote sensing observations of backscattering, such as C-band vertically polarized synthetic aperture radar (SAR) observations from the second European remote sensing (ERS-2) satellite, have the potential to measure moisture content in a near-surface layer of soil. However, SAR backscattering observations are highly dependent on topography, soil texture, surface roughness and soil moisture, meaning that soil moisture inversion from single frequency and polarization SAR observations is difficult. In this paper, the potential for measuring near-surface soil moisture with the ERS-2 satellite is explored by comparing model estimates of backscattering with ERS-2 SAR observations. This comparison was made for two ERS-2 overpasses coincident with near-surface soil moisture measurements in a 6 ha catchment using 15-cm time domain reflectometry probes on a 20 m grid. In addition, 1-cm soil moisture data were obtained from a calibrated soil moisture model. Using state-of-the-art theoretical, semi-empirical and empirical backscattering models, it was found that using measured soil moisture and roughness data there were root mean square (RMS) errors from 3·5 to 8·5 dB and r^2 values from 0·00 to 0·25, depending on the backscattering model and degree of filtering. Using model soil moisture in place of measured soil moisture reduced RMS errors slightly (0·5 to 2 dB) but did not improve r^2 values. Likewise, using the first day of ERS-2 backscattering and soil moisture data to solve for RMS surface roughness reduced RMS errors in backscattering for the second day to between 0·9 and 2·8 dB, but did not improve r^2 values. Moreover, RMS differences were as large as 3·7 dB and r^2 values as low as 0·53 between the various backscattering models, even when using the same data as input. These results suggest that more research is required to improve the agreement between backscattering models, and that ERS-2 SAR data may be useful for estimating fields-scale average soil moisture but not variations at the hillslope scale. Copyright © 2004 John Wiley & Sons, Ltd.

KEY WORDS remote sensing; soil moisture; active microwave; synthetic aperture radar; backscattering; backscattering models; soil roughness; ERS-2

INTRODUCTION

Recent advances in remote sensing have demonstrated the ability to measure the spatial variation of soil moisture content in the near-surface layer under a variety of topographic and land cover conditions using both active and passive microwave measurements. However, one important difference between spaceborne active and passive microwave remote sensing systems is the resolution of the resulting data. Active sensors have the capability to provide high spatial resolution, in the order of tens of metres, but are more sensitive to surface roughness, topographic features and vegetation than passive systems, meaning that soil moisture inversion from a single frequency, single polarization backscattering observation is difficult. On the other hand, the spaceborne passive systems can provide spatial resolutions only of the order of tens of kilometres, but with a higher temporal resolution.

* Correspondence to: Jeffrey P. Walker, Department of Civil and Environmental Engineering, The University of Melbourne, Parkville, Victoria 3010, Australia. E-mail: jiwalker@unimelb.edu.au

Received 25 May 2002
Accepted 3 March 2003

Most reviews suggest that near-surface soil moisture can be retrieved with sufficient accuracy from a multichannel (i.e. multiple frequencies or polarizations) synthetic aperture radar (SAR) instrument (e.g. Bindlish and Barros, 2000). However, all current spaceborne SAR instruments are single polarization, single frequency systems. To overcome this limitation, researchers have resorted to multiple images through time (e.g. Verhoest *et al*., 1998; Moran *et al*., 2000). This paper explores the potential to measure the moisture content of a near-surface soil layer using a minimum number of images from the single channel C-band SAR instrument on board the second European remote sensing (ERS-2) satellite. The ERS-2 backscattering measurements are compared with the predicted backscattering from several widely accepted state-of-the-art backscattering models (Fung *et al*., 1992; Oh *et al*., 1992, 1994) that are valid for the ERS-2 sensor configuration and roughness conditions of the field data. In addition to comparing measured and modelled backscattering values, and intercomparing the various backscattering models, this paper explores the potential for retrieving surface roughness parameters from simultaneous measurements of soil moisture and backscattering, and then using the retrieved surface roughness in future predictions of backscattering.

BACKGROUND TO ACTIVE MICROWAVE REMOTE SENSING

The fundamental basis of microwave remote sensing for soil moisture content is the contrast in dielectric properties of water and dry soil, and the relationship between the Fresnel reflection coefficient and dielectric constant. For a land surface, the target consists of the interface between air and soil. As the dielectric constant of the air is a known value, the reflection coefficient provides a measurement of the dielectric constant of the soil medium (Jackson *et al*., 1996).

As the scattering behaviour of a surface is governed by its geometrical and dielectric properties relative to the incident radiation, the variations in backscattering are influenced by soil moisture content (through the dielectric constant), topography, vegetation cover, surface roughness, observation frequency, wave polarization and incidence angle. A variation of relative dielectric constant between 3 and 30 (a shift in volumetric moisture content between approximately 2·5% and 50%, depending on frequency and soil texture) causes an 8 to 9 dB rise in backscatter coefficient for *vv* (vertical transmit vertical receive) polarization (Hoeben *et al*., 1997). This change in backscattering is almost independent of other parameters, such as incidence angle, frequency and surface roughness, but the total amount of backscattering is affected. The relationship between backscattering coefficient and dielectric constant is non-linear, having a higher sensitivity at low dielectric values.

Dielectric constant

Soil is a mixture of soil particles, air and both bound and free water (Ulaby *et al*., 1986). Microwave techniques for the measurement of soil moisture content rely on the clear distinction between the dielectric properties of water and those of the soil particles. The dielectric properties are measured by the dielectric constant ε, which is a complex number representing the response of a material to an applied electric field, such as an electromagnetic wave (Schmugge, 1985). This property consists of both real and imaginary parts by the relationship $\varepsilon = \varepsilon' + i\varepsilon''$, and is usually measured relative to that of free space (i.e. $\varepsilon_r = \varepsilon/\varepsilon_o$, where $\varepsilon_o = 8{\cdot}85 \times 10^{-12}$ farad m^{-1}).

The real (in-phase) component of ε determines the propagation characteristics of the electromagnetic wave in the material (i.e. its velocity), and the complex (out of phase) component determines the energy losses or absorption as the electromagnetic wave travels through the material (Schmugge, 1985; D'Urso *et al*., 1994; Engman and Chauhan, 1995; Bolognani *et al*., 1996; Zegelin, 1996), and is often referred to as the dielectric loss factor (Zegelin, 1996). The energy losses result from vibration and/or rotation of the water molecules (Wüthrich, 1997).

For dry soil particles, the real part of the relative dielectric constant ε_r' varies from a value of 2 to 5 (depending on soil bulk density) independent of frequency (Dobson and Ulaby, 1986), with an imaginary part ε_r'' typically less than 0·05 (Ulaby *et al*., 1996). In contrast, for free water the relative dielectric constant at

1 GHz and room temperature is approximately 80 for the real component and 4 for the imaginary component (Ulaby *et al*., 1996). It is this large difference that makes the measurement of soil moisture content by the microwave techniques possible.

Bound water has a lower dielectric constant than free water contained in the pore spaces, because its water molecules are adsorbed to the surfaces of particles and the dipoles are immobilized (Jackson and Schmugge, 1989; Njoku and Entekhabi, 1996). Hence, dielectric mixing models need to account for the contributions to dielectric constant from both bound and free water. Furthermore, as the dielectric constant of moist soil is proportional to the number of water dipoles per unit volume, the preferred measurement for soil moisture content in the mixing models is volumetric, rather than gravimetric (Dobson and Ulaby, 1986).

Topography

In addition to foreshortening and layover effects (Engman, 1991), topography affects the soil moisture inference from backscattering observations through the local incidence angle being different from that assumed for a flat surface (van Zyl, 1993). The cumulative effect is that the algorithm underestimates the soil moisture content and overestimates the surface roughness for surfaces tilted towards the radar, whereas it underestimates the roughness and overestimates the soil moisture for surfaces tilted away from the radar (Dubois *et al*., 1995). Lin *et al*. (1994) reports that *hh* (horizontal transmit horizontal receive) polarized signals appear to be most sensitive to the topographic effect.

The local incidence angle of each individual pixel may be calculated using the geometry of the remote sensing system and topographic information from a digital elevation model (DEM) by the expression (Robinson, 1966)

$$\cos\vartheta = \cos S \times \cos Z + \sin S \times \sin Z \times \cos(T - A) \tag{1}$$

where ϑ is the local incidence angle, S is the slope of the pixel, Z is the zenith angle of the remote sensing system defined as the angle between the radar and the normal to the horizontal surface at that position, T is the actual flight track of the remote sensing system, and A is the aspect angle of the pixel position. Variables T and A are defined to be zero to the north and increase counter clockwise.

Vegetation

Observations made with active microwave remote sensing are affected by vegetation cover by reducing the sensitivity of the return signal to soil moisture content. Vegetation above a soil surface absorbs and scatters part of the microwave radiation incident on it, as well as part of the reflected microwave radiation from the underneath soil surface. The amount of absorption is primarily a result of the water content of the vegetation (Schmugge, 1985), whereas the scattering is influenced by the vegetation shape and geometry (van de Griend and Engman, 1985).

Various authors (e.g. van de Griend and Engman, 1985; Brown *et al*., 1992; Schmulluis and Furrer, 1992; van Zyl, 1993) have noted that increasing the wavelength can generally diminish the effect of vegetation on the radar signal. Schmulluis and Furrer (1992) have shown that L-band (1 to 2 GHz) measurements will still yield good results under various agricultural crops, whereas for X- (8 to 12·5 GHz) and C-band (4 to 8 GHz), even a thin vegetation cover may distort the measurement. It has been shown, however, that C-band data can penetrate the vegetation canopy better when the vegetation is drier (Brown *et al*., 1992). The effect of vegetation is also greatly dependent upon the instrument angle of incidence and polarization (Ulaby *et al*., 1986), with the effect being small at low incidence angles (Wang *et al*., 1987). Ulaby *et al*. (1996) have shown that providing the vegetation cover is less than 15 cm, active microwave remote sensing can measure the volumetric moisture content of the near-surface soil layer with an root mean square (RMS) error of 3·5% at low microwave frequencies.

Surface roughness

Surface roughness is a major limiting factor for active microwave soil moisture remote sensing (Wang *et al*., 1987; Wüthrich, 1997) and simple correction procedures are difficult to develop (Jackson *et al*., 1996).

In many cases the effect of roughness may be equal to or greater than the effects of soil moisture content on the backscatter (Autret *et al*., 1989; Engman and Chauhan, 1995; Altese *et al*., 1996; Wüthrich, 1997), and in ploughed fields, the row structure generated by ploughing presents a periodic pattern that can further complicate data interpretation (Beaudoin *et al*., 1990; Giacomelli *et al*., 1995). Furthermore, the surface roughness of agricultural fields is not likely to remain constant between overpasses of more than 30 days (Wüthrich, 1997) owing to reductive tillage and weathering (Beaudoin *et al*., 1990), or between overpasses on different orbit tracks, which may have large differences in angle with respect to field direction (Wüthrich, 1997). However, in contrast to agricultural fields, the surface roughness of natural ecosystems does not change significantly over relatively short time periods (Sano *et al*., 1998).

Surface roughness characteristics generally have been described in terms of the RMS surface height, σ, roughness correlation length, l, and a correlation function. Of the roughness parameters, Jackson *et al*. (1997) suggests that RMS surface height is the most important. The method used to evaluate the roughness parameters generally has involved physically measuring the horizontal surface profile for a 1 to 2 m length at various locations over the site, using one of four methods. These methods have included: (i) inserting a thin metal plate vertically into the soil and then spraying with paint from an approximately horizontal direction; (ii) taking a photograph of the intersection of the ground surface with a gridded plate and digitizing the intersection; (iii) using a panel with drop pins; and (iv) using a laser profiler (Ulaby and Batliva, 1976; Ulaby *et al*., 1978; Troch *et al*., 1994; Wegmüller *et al*., 1994). These profiles generally are taken in several directions for each location (Troch *et al*., 1994). As there is no rule for choosing the spacing of roughness measurements along the profile, the suggestion of Ulaby *et al*. (1986) is often followed, using a spacing approximately equal to one-tenth of the free space wavelength.

Lin (1994) and Wang *et al*. (1987) have noted that the commonly used sampling techniques for measuring field surface roughness parameters required in microwave backscattering models are questionable, especially for smooth fields. This is because they have measurement scales of the order of a few metres, which is significantly smaller than the application scale when inferring near-surface soil moisture content from remote sensing observations. Moreover, it is questionable whether the correlation length can be estimated adequately from surface profiles of this length (Wang *et al*., 1987).

As there is no immediate hope of developing a surface roughness measurement technique with a measurement scale comparable to the application scale, and because it is too complex to develop a theory to bridge the gap between measurement and application scales, Lin (1994) and Wüthrich (1997) suggest an alternative data analysis scheme that uses field roughness measurements as a quality control measure only. This scheme involves collecting near-surface soil moisture content data by time domain reflectometry on a grid, and then solving for surface roughness using a microwave backscattering model. Comparison of the roughness characteristics evaluated can then be made with the field collected roughness data. However, a small error in soil moisture content can result in a large error in surface roughness, and using such to invert soil moisture again carries large uncertainties (Wüthrich, 1997). Altese *et al*. (1996) have found that for σ less than 1 cm, an error of 0·01 cm in the measurement of RMS height can imply an error in the inferred soil moisture content of up to 8% v/v, and for σ greater than 1 cm, an error of 0·01 cm in the measurement of RMS surface height can imply an error in the retrieved soil moisture content of only about 0·3% v/v.

Observation depth

The depth of soil over which the soil moisture can be inferred from remote sensing observations, known as the observation depth (Walker *et al*., 1997), is important for application of these measurements. However, there is little quantitative research in the literature on observation depth. On the basis of both experimental (Newton *et al*., 1982, 1983; Raju *et al*., 1995) and theoretical work (Wilheit, 1978; Schmugge and Choudhury, 1981; Ulaby *et al*., 1986), it is believed that the thickness of the near-surface soil layer that can effect such a response in a significant way for passive microwave remote sensing is between one-tenth and one-quarter of a wavelength. Although there is little quantitative evidence in the literature, it is believed that the thickness of

this layer is approximately the same for both active and passive microwave remote sensing (Schmugge 1985; Engman and Chauhan, 1995; van Oevelen, 1998). Observation depth is usually discussed only in relation to wavelength, but the depth of soil over which microwave instruments are sensitive is also dependent on the soil moisture content. As the soil moisture content is increased, the observation depth decreases (Njoku and Kong, 1977; Newton *et al*., 1982; Arya *et al*., 1983; Bruckler *et al*., 1988; Engman and Chauhan, 1995; Raju *et al*., 1995). The observation depth is also noted to be a function of incidence angle, wave polarization, surface roughness and vegetation cover (Arya *et al*., 1983) and soil moisture profile shape (Njoku and Entekhabi, 1996).

BACKSCATTERING MODELS

The backscattering coefficient σ^{o}, which is a unitless quantity representing the radar cross-section (m^2) of a given pixel on the ground per unit physical area of that pixel (m^2), may exhibit a wide dynamic range, and therefore is often presented in decibels (Ulaby *et al*., 1996). To convert the backscattering values obtained to decibels, the following relationship is used

$$\sigma^{o}_{dB} = 10 \log_{10} \sigma^{o} \tag{2}$$

All published backscattering models having applicability to the ERS-2 SAR data were used in this study. These were: (i) the empirical model (EM) of Oh *et al*. (1992); (ii) the theoretical integral equation model (IEM) of Fung *et al*. (1992); and (iii) the semi-empirical model (SEM) of Oh *et al*. (1994). The models of Dubois *et al*. (1995), Chen *et al*. (1995) and Shi *et al*. (1997) could not be used, as they were not valid for the data used in this paper, owing to observation frequency, incidence angle, surface roughness and or surface roughness correlation length limitations. The backscattering models presented below give the backscattering coefficient in linear units.

Empirical model (EM)

To establish a useful empirical relationship for inversion of soil moisture from backscattering observations, it is necessary to have a great number of experimental measurements in order to derive general statistical laws (Oh *et al*., 1992). However, empirical backscattering models found in the literature generally are derived from specific data sets and are mostly only valid in certain regions of roughness, frequency, incidence angle and soil moisture content. Furthermore, empirical backscattering models may not be applicable for data sets other than those used in their development (Chen *et al*., 1995; Dubois *et al*., 1995). The main advantage of empirical backscattering models over theoretical backscattering models is that many natural surfaces do not fall into the validity regions of the theoretical backscattering models, and even when they do, the available backscattering models fail to provide results in good agreement with experimental observations (Oh *et al*., 1992).

The empirical backscattering model of Oh *et al*. (1992) is based on L-, C- and X-band spectrometer data, with incidence angles varying from 10° to 70°. The surface roughness and soil moisture content cover the ranges $0{\cdot}1 < k_o\sigma < 6{\cdot}0$, $2{\cdot}6 < k_o l < 19{\cdot}7$ and $0{\cdot}09 < \theta < 0{\cdot}31$, where k_o is the free space wave number given by $k_o = 2\pi/\lambda_o$, λ_o is the free space wavelength and θ is the volumetric soil moisture content. As backscattering from smooth surfaces includes a strong contribution as a result of the coherent (specular) backscattering component that exists at angles close to normal incidence, the range of applicability of the backscattering model does not include the angular range below 20° for smooth surfaces. This backscattering model is presented as

$$\sigma^{o}_{vv} = \frac{g \cos^3 \vartheta}{\sqrt{p}} [\Gamma_v + \Gamma_h] \tag{3}$$

where

$$\sqrt{p} = 1 - \left(\frac{2\vartheta}{\pi}\right)^{\frac{1}{3\Gamma_0}} \exp(-k_o\sigma) \tag{4a}$$

$$g = 0{\cdot}7[1 - \exp(-0{\cdot}65(k_o\sigma)^{1{\cdot}8})] \tag{4b}$$

$$\Gamma_v = \left|\frac{\varepsilon_r \cos\vartheta - \sqrt{\varepsilon_r - \sin^2\vartheta}}{\varepsilon_r \cos\vartheta + \sqrt{\varepsilon_r - \sin^2\vartheta}}\right|^2 \tag{5a}$$

$$\Gamma_h = \left|\frac{\cos\vartheta - \sqrt{\varepsilon_r - \sin^2\vartheta}}{\cos\vartheta + \sqrt{\varepsilon_r - \sin^2\vartheta}}\right|^2 \tag{5b}$$

$$\Gamma_0 = \left|\frac{1 - \sqrt{\varepsilon_r}}{1 + \sqrt{\varepsilon_r}}\right|^2 \tag{5c}$$

and Γ_v and Γ_h are the vertical and horizontal Fresnel reflectivities and Γ_0 is the Fresnel reflectivity at nadir.

Theoretical model (IEM)

Theoretical backscattering models are derived from application of the theory of electromagnetic wave scattering from a randomly rough conducting surface (Fung *et al*., 1992). These backscattering models are preferable to empirical and semi-empirical backscattering models, as they provide site-independent relationships that are valid for different sensor configurations, and take into account the effect of different surface parameters on backscattering (Altese *et al*., 1996). Using simplifying assumptions, theoretical backscattering models with different ranges of validity may be obtained.

The standard theoretical backscattering models are the Kirchhoff models (KM), which consists of the geometrical optics model (GOM) and physical optics model (POM), and the small perturbation model (SPM) (Ulaby *et al*., 1986). In a broad sense, the GOM is best suited for very rough surfaces, the POM is suited for surfaces with intermediate roughness, and the SPM is suited for surfaces with small roughness and short roughness correlation lengths (Engman and Chauhan, 1995).

The integral equation model (IEM) was developed by Fung *et al*. (1992), and is shown to unite the KM and SPM, hence making it applicable to a wider range of roughness conditions or frequencies. In its complete version, the model describes the backscattering behaviour of a random rough bare surface without any limitation on the roughness scale or frequency range, and accounts for both single and multiple surface scattering of a conducting surface. Because of its complexity, it is not practical to use the complete version of the IEM and in applications approximate solutions are usually considered.

Altese *et al*. (1996) have used an approximate version of the IEM, which is valid for surfaces with small to moderate surface RMS heights. The validity expression for this approximate version is $k_o\sigma < 3$. Altese *et al*. (1996) used only the single scattering component of the IEM and made further simplifying assumptions by using only the real part of the relative dielectric constant and assuming that the surface correlation function is isotropic and can be represented by either the Gaussian or exponential models.

As most natural terrains have a small RMS surface slope, it has been suggested by Fung *et al*. (1992) that single scattering terms should dominate over multiple scattering terms in most situations. The conditions under which significant multiple scattering has been found to occur are: (i) normalized surface height $k_o\sigma > 1$; and (ii) surface RMS slope $\gamma > 0{\cdot}5$ (Hsieh and Fung, 1997) where $\gamma = \sigma/l$.

The approximate version of the IEM used by Altese *et al*. (1996) has been used successfully by Su *et al*. (1997) to estimate volumetric soil moisture content in bare fields during the European Multi-sensor Airborne

Campaign 1994 (EMAC'94), and is given as

$$\sigma_{vv}^{o} = \frac{k_o^2}{2}\exp(-2k_{zo}^2\sigma^2)\sum_{n=1}^{\infty}\sigma^{2n}|I_{vv}^n|^2\frac{W^n(-2k_{xo},0)}{n!} \tag{6}$$

where

$$I_{vv}^n = (2k_{zo})^n f_{vv}\exp(-\sigma^2 k_{zo}^2) + \frac{k_{zo}^n[F_{vv}(-k_{xo},0)+F_{vv}(k_{xo},0)]}{2} \tag{7a}$$

$$f_{vv} = \frac{2R_v}{\cos\vartheta} \tag{7b}$$

$$F_{vv}(-k_{xo},0)+F_{vv}(k_{xo},0) = \frac{2\sin^2\vartheta(1+R_v)^2}{\cos\vartheta}\times\left[\begin{array}{l}\left(1-\frac{1}{\varepsilon_r}\right)+\\ \frac{\mu_r\varepsilon_r-\sin^2\vartheta-\varepsilon_r\cos^2\vartheta}{\varepsilon_r^2\cos^2\vartheta}\end{array}\right] \tag{7c}$$

$$R_v = \frac{\varepsilon_r\cos\vartheta-\sqrt{\varepsilon_r-\sin^2\vartheta}}{\varepsilon_r\cos\vartheta+\sqrt{\varepsilon_r-\sin^2\vartheta}} \tag{8a}$$

$$R_0 = \frac{1-\sqrt{\varepsilon_r}}{1+\sqrt{\varepsilon_r}} \tag{8b}$$

$$W^n(K) = \left(\frac{l}{n}\right)^2\left[1+\left(\frac{Kl}{n}\right)^2\right]^{-1\cdot5} \tag{9}$$

and f_{vv} is the Kirchhoff coefficient, F_{vv} is the complementary field coefficient, R_v is the vertical Fresnel reflection coefficient, R_0 is the Fresnel reflection coefficient at nadir, k_{zo} is the z component of the free space wave number given by $k_{zo} = k_o\cos\vartheta$, k_{xo} is the x component of the free space wave number given by $k_{xo} = k_o\sin\vartheta$ and μ_r is the relative magnetic permeability, which is usually equal to unity for soil, because soil rarely contains significant amounts of ferromagnetic components (Roth *et al*., 1990). Variable W^n is the roughness spectrum of the surface related to the nth power of the two-parameter surface correlation function $\rho(\xi,\varsigma)$ by the Fourier transformation, and is usually simplified to a single parameter isotropic case (Fung, 1994). Altese *et al*. (1996) have shown that the behaviour of the IEM is highly dependent on the choice of the correlation function. The roughness spectrum Fourier transform of the nth power of the exponential correlation function is used in this study (Equation 9) as Wegmüller *et al*. (1994) have shown that the exponential correlation function usually gives a better agreement to the observed correlation function than the Gaussian correlation function in agricultural fields.

There are two approximations that have been made to the local angle in the Fresnel reflection coefficient R_v to be used in the Kirchhoff coefficient f_{vv} (Fung, 1994). One approximation replaces the local angle by the incident angle and the other by the angle along the specular direction. The local angle in the Fresnel reflection coefficients in the complementary field coefficients F_{vv} is always approximated by the incident angle. Fung (1994) has shown that the approximation by the incident angle is good for the low to intermediate frequency region, whereas the other approximation is good in the high frequency region. Thus, it has been proposed by Fung (1994) that for $k_o\sigma k_o l < a\sqrt{\varepsilon_r}$, ϑ is the incident angle, and for $k_o\sigma k_o l > a\sqrt{\varepsilon_r}$, ϑ is equal to 0°, where a is 200 for an exponential surface roughness correlation function.

Theoretical models can predict reasonably well the general trend of backscattering coefficient in response to changes in roughness or soil moisture content. However, because of their complexity or the restrictive assumptions made when deriving them, it has been reported by various researchers (Oh *et al*., 1992; Dubois and van Zyl, 1994; Dubois *et al*., 1995) that they can rarely be used to invert data measured from natural surfaces,

owing to failure of satisfying validity regions or in providing results in good agreement with experimental observations.

Semi-empirical model (SEM)

Semi-empirical backscattering models are an improvement to empirical backscattering models in so much as they start from a theoretical background and then use simulated or experimental data sets to simplify the theoretical backscattering model. Alternatively, they use simulated data from a theoretical backscattering model to derive an empirical backscattering model that describes the backscattering response for a wide range of surface conditions. The main advantage of these backscattering models is that they are not expected to have the site-specific problems commonly associated with empirical backscattering models derived from a limited number of observations.

Among the first semi-empirical backscattering models was that of Oh *et al*. (1994). This model is based on existing theoretical backscattering models (SPM and KM) in conjunction with extensive experimental data, and is an extension of their empirical model (Equation 3) to include both the magnitude and phase of the backscattering. The experimental data that was used to solve for the unknown constants of the expression were collected from a truck-mounted L-, C- and X-band polarimetric scatterometer over a range of incidence angles from 10° to 70°. The expression chosen for the vv polarized backscattering was

$$\sigma^{o}_{vv} = 13{\cdot}5 \exp(-1{\cdot}4(k_o\sigma)^{0{\cdot}2}) \frac{1}{\sqrt{p}} \Gamma_h (k_o\sigma)^2 (\cos\vartheta)^{3{\cdot}25-0{\cdot}05k_o l} \exp(-(2k\sigma\cos\vartheta)^{0{\cdot}6}) W \tag{10}$$

where

$$\sqrt{p} = 1 - \left(\frac{2\vartheta}{\pi}\right)^{\frac{0{\cdot}314}{\Gamma_0}} \exp(-k_o\sigma) \tag{11}$$

$$W = \frac{(k_o l)^2}{1 + (2{\cdot}6k_o l \sin\vartheta)^2} \left[1 - 0{\cdot}71 \frac{1 - 3(2{\cdot}6k_o l \sin\vartheta)^2}{[1 + (2{\cdot}6k_o l \sin\vartheta)^2]^2}\right] \tag{12}$$

and W is the roughness spectrum corresponding to a quadratic exponential correlation function, which was found by Oh *et al*. (1994) to be the form of the correlation function that best describes the roughness of natural fields.

Dielectric constant mixing model

The model of Peplinski *et al*. (1995) is currently amongst the most commonly used soil–water–air dielectric mixing models, being a compromise between the complexity of the theoretical models and the simplicity of the empirical models. Furthermore, this mixing model has the widest validity range in terms of observation frequency and accounts for the most important factors, including observation frequency, soil texture and soil temperature. The real component of the dielectric constant as determined by this model is presented below in terms of the volumetric soil moisture fraction, θ, soil bulk density, ρ_b (g cm^{-3}), soil specific density, ρ_s (c.2·66 g cm^{-3}), and an empirically determined constant $\upsilon = 0{\cdot}65$.

$$\varepsilon'_r = \left[1 + \frac{\rho_b}{\rho_s}(\varepsilon_s^{\upsilon} - 1) + \theta^{\beta'}\varepsilon'^{\upsilon}_{fw} - \theta\right]^{\frac{1}{\upsilon}} \tag{13}$$

where β' is an empirically determined soil type constant expressed as a function of the sand (S) and clay (C) mass fractions by

$$\beta' = 1{\cdot}2748 - 0{\cdot}519S - 0{\cdot}152C \tag{14}$$

The quantity $\varepsilon'_{\mathrm{fw}}$ is the real parts of the relative dielectric constant of free water given by

$$\varepsilon'_{\mathrm{fw}} = \varepsilon_{\mathrm{w}\infty} + \frac{\varepsilon_{\mathrm{wo}} - \varepsilon_{\mathrm{w}\infty}}{1 + (2\pi f \tau_{\mathrm{w}})^2} \tag{15}$$

where $\varepsilon_{\mathrm{w}\infty} = 4{\cdot}9$ is the high frequency limit of $\varepsilon'_{\mathrm{fw}}$ and f is the observation frequency in hertz. The relaxation time for water τ_{w} and the static dielectric constant of water $\varepsilon_{\mathrm{wo}}$ are given as a function of soil temperature T (°C) by (Ulaby *et al*., 1986)

$$2\pi\tau_{\mathrm{w}}(T) = 1{\cdot}1109 \times 10^{-10} - 3{\cdot}824 \times 10^{-12}T + 6{\cdot}938 \times 10^{-14}T^2 - 5{\cdot}096 \times 10^{-16}T^3 \tag{16a}$$

$$\varepsilon_{\mathrm{wo}}(T) = 88{\cdot}045 - 0{\cdot}4147T + 6{\cdot}2958 \times 10^{-4}T^2 + 1{\cdot}075 \times 10^{-5}T^3 \tag{16b}$$

The relative dielectric constant of the soil solids, ε_s, is given by the relationship

$$\varepsilon_{\mathrm{s}} = (1{\cdot}01 + 0{\cdot}44\rho_{\mathrm{s}})^2 - 0{\cdot}062 \tag{17}$$

This is the dielectric mixing model used in this paper.

DATA

In this paper, backscattering measurements from the ERS-2 SAR (corrected for variation in zenith viewing angle) are compared with predicted backscattering for the 'Nerrigundah' experimental catchment located in a temperate region of eastern Australia. A detailed description of the entire Nerrigundah data set is given in Walker *et al*. (2001), so only the pertinent details are given here.

ERS-2 satellite data

The second European remote sensing (ERS-2) satellite was launched in 1995 and carried on board various advanced instruments for Earth observation. Of interest for hydrological applications is the active microwave instrument (AMI), which comprises two separate radars: a SAR and a wind scatterometer. The AMI-SAR instrument operates at C-band (5·3 GHz) with a vv polarization, the same configuration as ERS-1. In SAR image mode it provides high resolution two-dimensional images with a spatial resolution of 26 m in range and between 6 and 30 m in azimuth. The ERS precision radar images are 3-look images corrected for the in-flight SAR antenna pattern and compensated for range spreading loss with a pixel size of 12·5 m ×12·5 m. The satellite has a swath of 100 km to the right side of the satellite track. The mid-swath zenith angle (Z_{ref}) of the system in normal operation mode is 23°. The ERS-2 satellite has a Sun-synchronous orbit of 785 km with a 35-day repeat cycle and is continuing to outlive its design life.

To derive the radar backscattering coefficient from the ERS-2 SAR PRI (PRecision Image) product and correct for variation in zenith angle across the satellite swath, it is necessary to apply the equations set out in Laur *et al*. (1998). Using the simplified derivation method and using an area of interest as the individual pixel to be calibrated, the equation simplifies to

$$\sigma^{\mathrm{o}} = DN^2 \times \frac{1}{K}\frac{\sin Z}{\sin Z_{\mathrm{ref}}} \tag{18}$$

where DN is the digital number for the pixel from the PRI image, K is the calibration constant and Z is the zenith angle for the pixel, which varies with position across-track in the satellite swath.

Two ERS-2 SAR PRI images are analysed in this paper (Figure 1). These images were obtained as part of a 1-month intensive field campaign in the Nerrigundah catchment and are for 6 September and 22 September 1997 (Julian days 249 at 12 : 59 and 265 at 12 : 56, Australian eastern standard time). Although the satellite

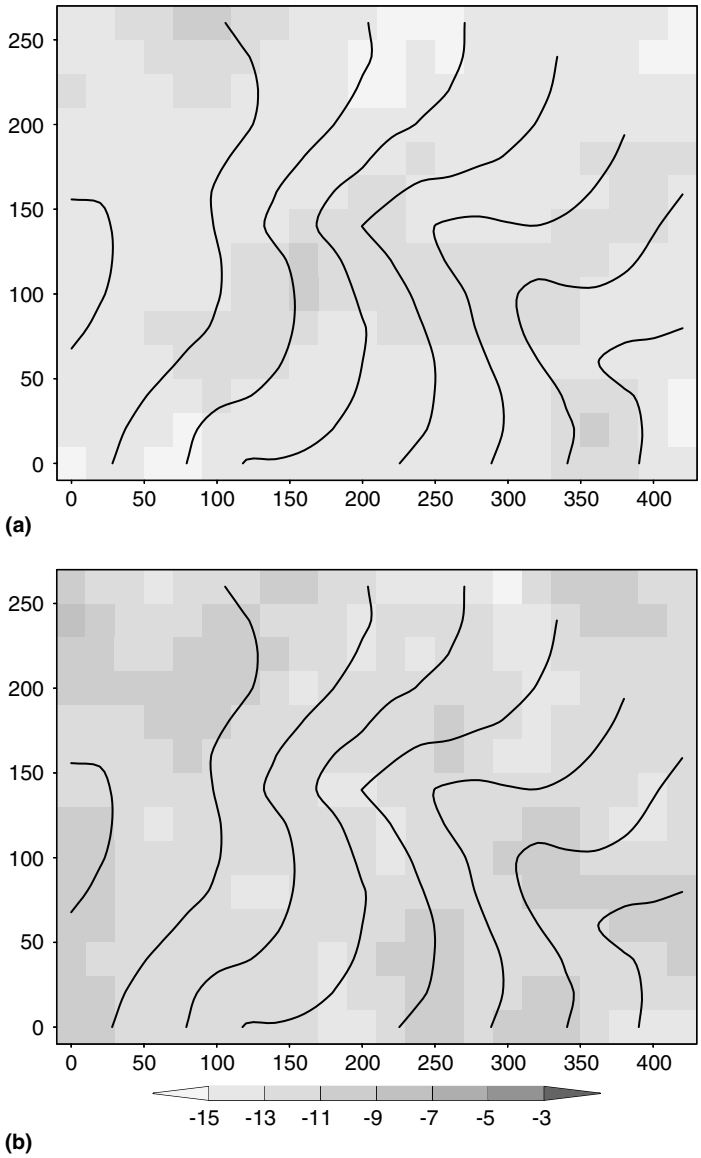

Figure 1. ERS-2 backscattering data (dB) on Julian day of year (a) 249 and (b) 265 after applying a 3 × 3 filter. Contour lines are elevation with an interval of 5 m

has a 35-day repeat orbit, owing to overlapping of satellite orbit tracks it was possible to obtain two images within a month.

Nerrigundah catchment data

The Nerrigundah catchment is located approximately 11 km north-west of Dungog, New South Wales, Australia (32°19′ south; 151°43′ east). The catchment runs east to west with a relief of 27 m and a catchment area of 6 ha. Hill slopes are typically 11% with a range from 3% to 22%, and the main drainage line has an average slope of 9% with a range from 1% to 17%. The catchment was vegetated with low pasture for grazing of beef cattle (Figure 2).

Figure 2. Photograph of the Nerrigundah study catchment

The site was instrumented to monitor evapotranspiration, precipitation and soil moisture variation throughout the entire catchment from 22 August 1997 until 20 October 1998, with an intensive field campaign from 27 August 1997 until 22 September 1997. During the intensive field campaign, near-surface soil moisture measurements were made using 15-cm time domain reflectometry (TDR) probes on a 20 m regular grid every 2 to 3 days, to replicate remote sensing observations of soil moisture, with the mapping taking 6 to 8 h. The ERS-2 overpasses were coincident with two of these soil moisture mappings (Figure 3). Soil texture and soil bulk density was determined by laboratory analysis of minimally disturbed soil samples taken from 19 locations throughout the catchment. Topographic variations in the incidence angle were corrected using Equation (1) and an accurate DEM of the Nerrigundah catchment. The change in zenith angle across the image and between the two overpass dates was accounted for by Equation (18), correcting to the equivalent value for a zenith angle of 23°.

Surface roughness measurements were made for each of the satellite overpasses using a 1-m-long drop pin profiler with a pin separation of 25 mm. Two sets of measurements were made in, north–south, east–west, and north-east–south-west directions, at each of five locations; the top of the catchment, the bottom of the catchment, either side of the catchment midway, and in the centre of the catchment in the main drainage line. A visual inspection of the Nerrigundah catchment indicated that the spatial distribution of surface roughness appeared uniform, apart from the main drainage line and steeper portions of the site. These portions were slightly rougher as a result of cattle grazing. However, there was a wide variation in the roughness measurements, even for consecutive surface roughness profile segments at the same site, for the same direction, and for the same day. Hence, roughness measurements for a given measurement site were averaged prior to interpolation throughout the catchment.

Although the SAR signal at C-band is influenced by only the top centimetre or so of soil moisture content (Walker *et al*., 1997) and TDR measurements were made over the top 15-cm, providing the soil moisture is relatively wet or relatively dry, the 15-cm measurements should be indicative of the soil moisture content in the top few centimetres (Western *et al*., 1997). However, as shallower soil moisture measurements were not made, the 15-cm soil moisture data were supplemented with 1-cm soil moisture estimates (Figure 4) from the soil moisture modelling presented in Walker *et al*. (2002). In this study, the soil moisture model was calibrated to 10 months of soil moisture profile data collected at 13 locations throughout the 6 ha catchment, and evaluated against the soil moisture profile measurements that were made on the same days as near-surface measurements during the intensive field campaign.

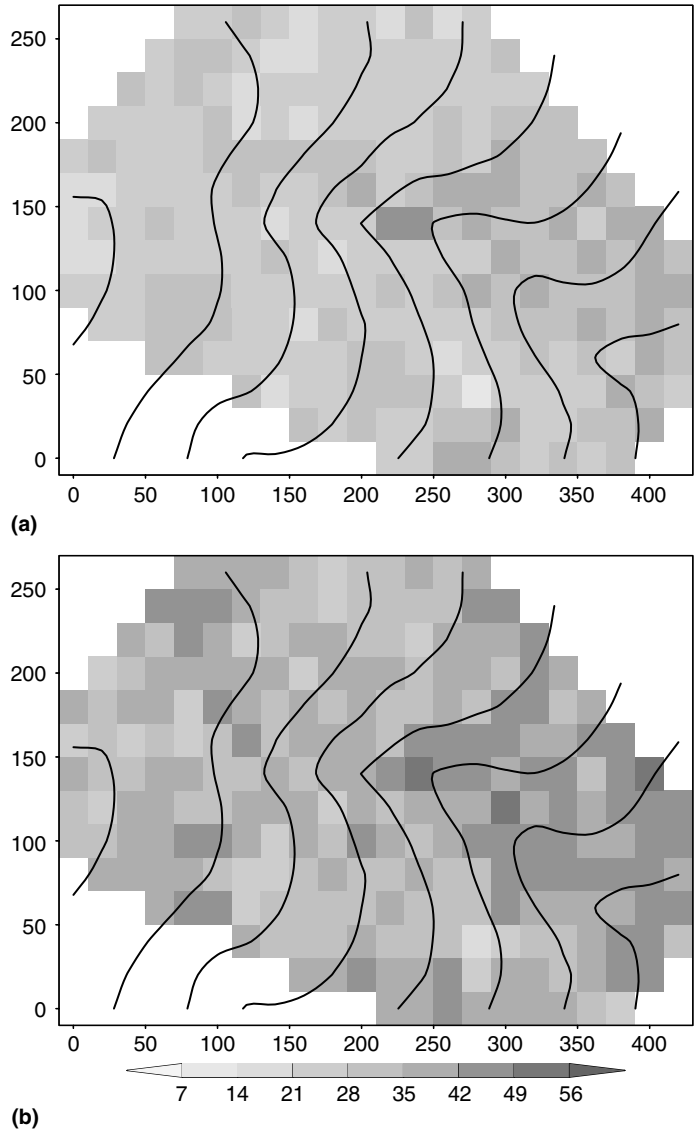

Figure 3. Soil moisture measurements (% v/v) of top 15 cm using time domain reflectometry on Julian day (a) 249 and (b) 265. Contour lines are elevation with an interval of 5 m

FIELD EVALUATION

The field evaluation of soil moisture measurement from ERS-2 backscattering observations was made in three stages; (i) an intercomparison of the three backscattering models, (ii) an evaluation of the model predicted backscattering using only measured inputs of soil roughness, and (iii) an evaluation of the model predicted backscattering when calibrating the RMS surface roughness parameter. First, a scatter plot of ERS-2 backscattering was compared with measured and modelled soil moisture content (Figure 5). This figure indicates a weak relationship between the observed backscatter and the measured soil moisture content, but this does not account for spatial variations in soil properties and terrain induced variations in incidence angle, which are accounted for in the backscattering models. However, there is a slight improvement as the ERS-2

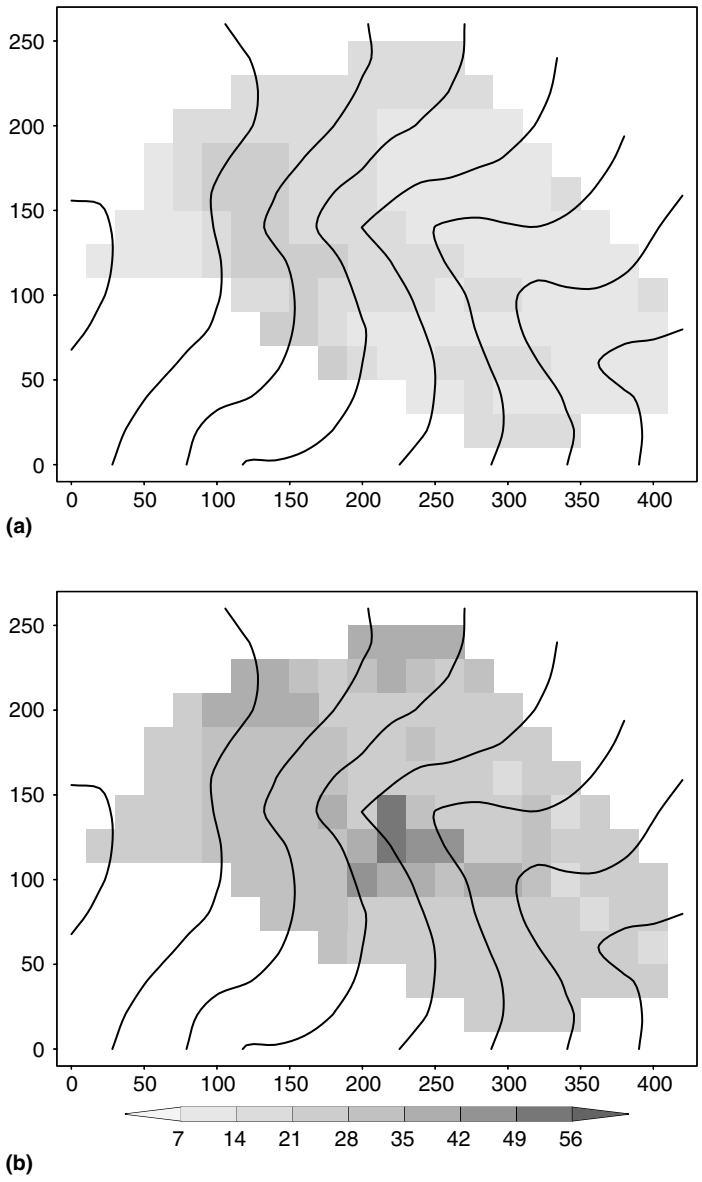

Figure 4. Soil moisture estimates (% v/v) of top 1 cm using a soil moisture model on Julian day (a) 249 and (b) 265. Contour lines are elevation with an interval of 5 m

backscattering data is filtered with an increasing filter size. Use of modelled soil moisture in place of measured soil moisture gives similarly poor results.

Model intercomparison

Using the same input of measured soil moisture, soil texture and surface roughness data (so much as possible), predicted backscattering was derived for each of the 2 days using the three different backscattering models presented; theoretical (IEM), empirical (EM) and semi-empirical (SEM). Scatter plots of the model intercomparison are given in Figure 6 and the results summarized in Table I through the RMS difference in

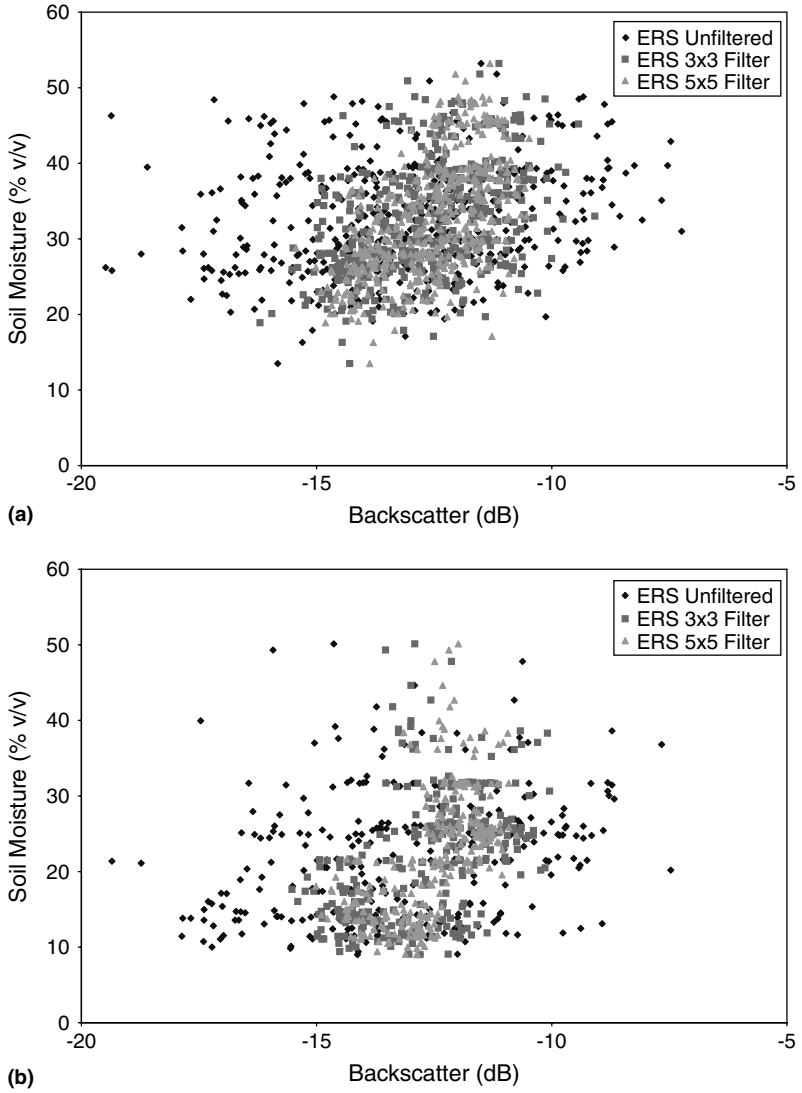

Figure 5. ERS-2 backscattering with various levels of filtering is compared with (a) soil moisture measurements of the top 15 cm using time domain reflectometry and (b) soil moisture estimates of the top 1 cm using a soil moisture model for Julian days 249 and 265

backscattering between the three models and the r^2 value (sample size is 238). The figure shows that all three models have similar backscattering responses on the two different days, but with a slight shift upward and to the right on Julian day 265 owing to the slightly wetter conditions on that day.

This intercomparison reveals a surprisingly large variation between the three models, with an RMS difference as large as 3·7 dB and r^2 as low as 0·53. The IEM and EM models had differences as large as 6·5 dB, corresponding to more than half the sensitivity in backscattering coefficient to change in soil moisture from dry to wet. The greatest RMS difference in backscattering between the three models was for the IEM and EM, and the lowest r^2 was between the SEM and EM. However, the least RMS difference in backscattering was for the SEM and EM and the highest r^2 was between the IEM and SEM. Moreover, the IEM shows a bias as compared with the EM and SEM.

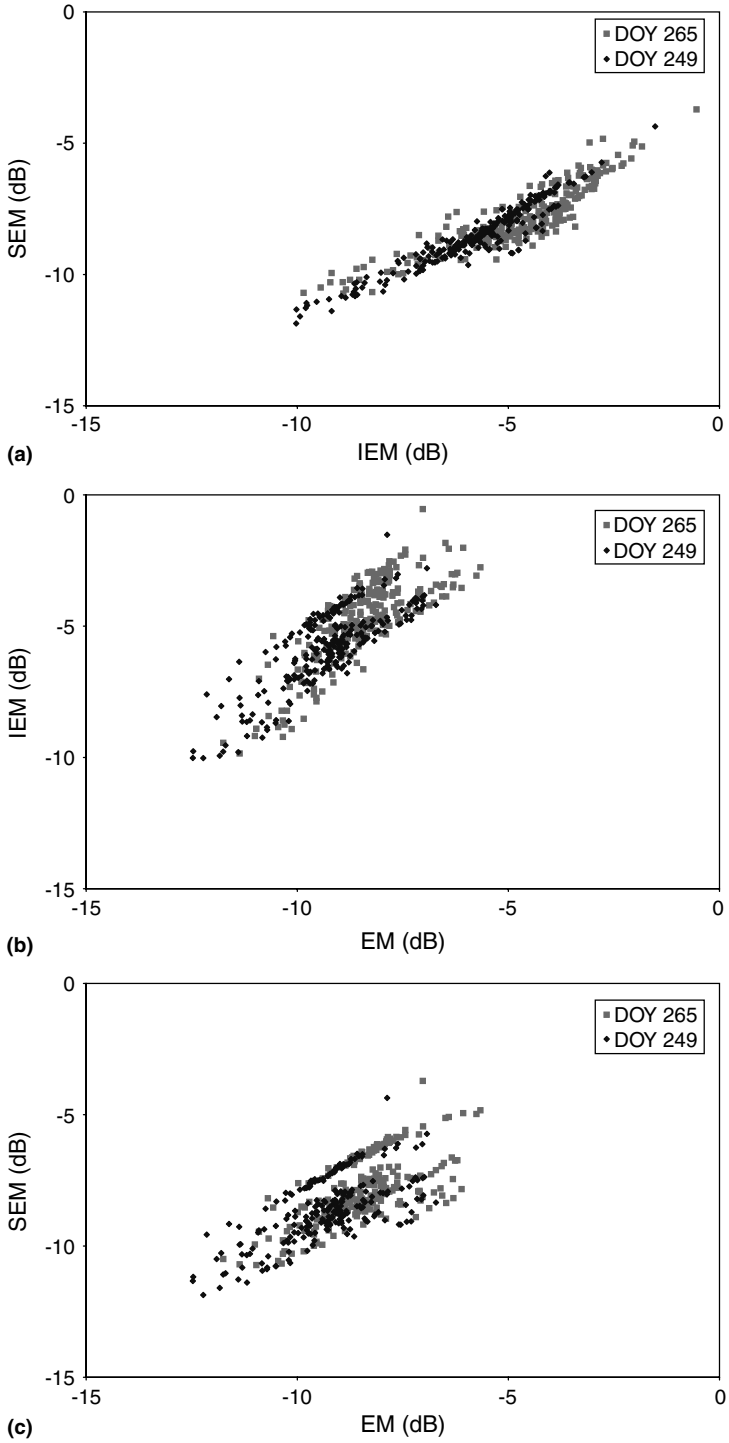

Figure 6. Comparison of the three backscattering model predictions with the same input data for soil moisture, soil properties and surface roughness for Julian days 249 and 265

Table I. Summary of RMS (dB) and r^2 values between the three backscattering model predictions with the same input data for soil moisture, soil properties and surface roughness

Model 1	Model 2	Julian day 249		Julian day 265	
		RMS	r^2	RMS	r^2
IEM	SEM	2·9	0·91	3·1	0·79
IEM	EM	3·7	0·75	3·7	0·64
SEM	EM	1·2	0·66	1·1	0·53

These results were not entirely surprising, as one would expect the largest discrepancy between theoretical and empirical models, with semi-empirical models somewhere in between. However, the magnitude of RMS differences and the poor r^2 values were somewhat surprising. This suggests that there is still a significant amount of work required with the development of backscattering models in order to accurately predict the backscattering response to soil moisture and roughness and obtain some consistency between models.

Model evaluation: measured roughness

In the first phase of model evaluation, the measured surface roughness and soil texture data were used as direct input to the backscattering models, together with both the field measured and model estimated soil moisture data (used separately). Figure 7 shows the predicted backscattering on Julian day 265 for each of the three backscattering models using both measured and modelled soil moisture. This figure shows a wide range in predicted backscattering for the different soil moisture input, as well as between the different backscattering models. This figure is to be compared with the observed ERS-2 backscattering in Figure 1b.

A summary of the RMS errors and r^2 values between each of the predicted backscattering values and the ERS-2 observations is given in Tables II and III for Julian days 249 and 265 respectively (sample size is 238 for measured soil moisture and 146 for modelled soil moisture). Although scatter plots are not included for the summary statistics given in Tables II to V, the plots given in Figures 5 and 6 are typical of all other results. Comparison of these two tables shows comparable RMS errors for the two different days (2·2 to 8·4 dB), although there were greater, yet still insignificant (less than 0·25), r^2 values for the first day. It is possible that this lower r^2 for the second day (less than 0·17) was a result of the 7·5 mm of rainfall that fell uniformly over the catchment 3 days before the second overpass of the ERS-2 satellite. Moreover, the models are more correlated to each other (Table I and Figure 6) than they are to the data (Table II).

The IEM backscattering prediction had the greatest RMS error (as high as 8·4 dB), whereas the EM had the lowest RMS error (as low as 2·2 dB; 5·1 dB for the comparable backscattering prediction to the IEM

Table II. Summary of RMS (dB) and r^2 values for the three backscattering models and three levels of filtering on ERS-2 SAR data for Julian day 249 with measured RMS surface roughness

Model	Depth (cm)	Unfiltered		3 × 3 filter		5 × 5 filter	
		RMS	r^2	RMS	r^2	RMS	r^2
IEM	1	6·6	0·08	5·8	0·22	5·7	0·25
	15	8·4	0·04	7·8	0·18	7·7	0·21
EM	1	3·4	0·10	2·4	0·22	2·2	0·22
	15	5·1	0·03	4·4	0·12	4·2	0·18
SEM	1	4·1	0·07	3·2	0·15	3·1	0·17
	15	5·7	0·04	5·1	0·16	5·0	0·18

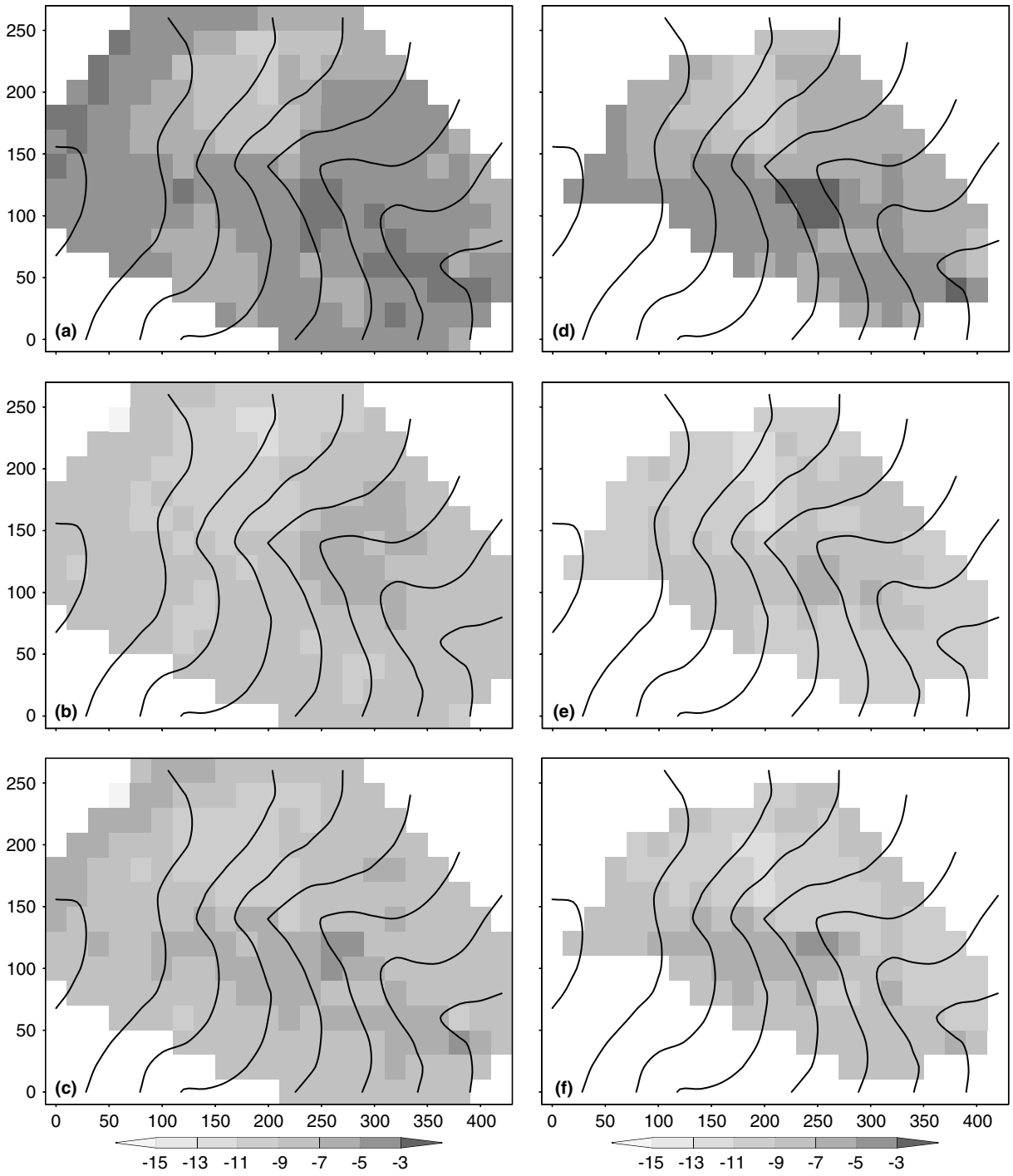

Figure 7. Predicted backscattering for Julian day 265 using measured RMS surface roughness with: measured soil moisture and (a) IEM, (b) EM and (c) SEM backscattering models; modelled soil moisture and (d) IEM, (e) EM and (f) SEM backscattering models (dB). Contour lines are elevation with an interval of 5 m

Table III. Summary of RMS (dB) and r^2 values for the three backscattering models and three levels of filtering on ERS-2 SAR data for Julian day 265 with measured RMS surface roughness

Model	Depth (cm)	Unfiltered		3 × 3 filter		5 × 5 filter	
		RMS	r^2	RMS	r^2	RMS	r^2
IEM	1	7·4	0·00	6·6	0·00	6·5	0·06
	15	8·2	0·00	7·3	0·06	7·2	0·17
EM	1	4·1	0·00	3·1	0·00	2·9	0·00
	15	4·8	0·00	3·7	0·02	3·5	0·04
SEM	1	4·7	0·01	3·8	0·02	3·6	0·00
	15	5·3	0·00	4·3	0·00	4·1	0·07

Table IV. Summary of RMS (cm), r^2 and maximum difference (cm) between the measured and retrieved RMS surface roughness for Julian day 249 using both measured and modelled soil moisture in the three backscattering models

Model	Depth (cm)	RMS	r^2	Maximum
IEM	1	0·44	0·21	0·97
	15	0·49	0·00	1·03
EM	1	0·27	0·61	0·68
	15	0·39	0·00	0·85
SEM	1	0·35	0·45	0·87
	15	0·48	0·00	0·97

Table V. Summary of RMS (dB) and r^2 values for the three backscattering models and three levels of filtering on ERS-2 SAR data for Julian day 265 with inverted RMS surface roughness from Julian day 249 and 5 × 5 filter on ERS-2 data

Model	Depth (cm)	Unfiltered		3 × 3 filter		5 × 5 filter	
		RMS	r^2	RMS	r^2	RMS	r^2
IEM	1	2·8	0·02	1·5	0·09	1·	0·16
	15	2·4	0·01	1·2	0·09	0·9	0·17
EM	1	2·7	0·00	1·5	0·00	1·3	0·00
	15	2·5	0·00	1·4	0·00	1·2	0·00
SEM	1	2·6	0·00	1·4	0·00	1·2	0·00
	15	2·5	0·00	1·4	0·00	1·2	0·00

RMS error above). This is consistent with the model intercomparison results, where the IEM and EM had the greatest RMS difference, indicating that the EM gives the best prediction of backscattering, even when there is no calibration of the input parameters. The IEM yielded slightly higher r^2 values than the EM, but owing to the low values (less than 0·25) this is not significant, and indicates that the noise in ERS-2 data is too great to enable measurement of soil moisture variations at the hillslope scale. However, the increasing r^2 value with increasing filter size (100 m × 100 m for the 5 × 5 filter) suggests that measurement of soil moisture variations at the plot scale may be possible with the ERS-2 satellite, even though hillslope variations are not. Filtering of the ERS-2 data also had the effect of decreasing the RMS error, meaning that averaging of SAR data gives a better estimate of the soil mean response.

When the measured soil moisture was replaced with modelled soil moisture, the RMS errors were slightly reduced (by 0·5 to 2 dB) and the r^2 values were slightly increased for some situations. This is because the

modelled soil moisture depth is more representative of the ERS-2 observation depth, with the reduction in RMS errors a reflection of the drier soil moisture values for a shallower soil layer than that measured in the field.

Model evaluation: retrieved roughness

In the second phase of evaluation, the RMS surface roughness was retrieved by calibrating the predicted backscattering to the ERS-2 data from Julian day 249, using the soil moisture data as input. The surface roughness correlation length was taken from the field measurements and the RMS surface roughness retrieved. The retrieved RMS surface roughness was then used with the soil moisture data on Julian day 265 to predict the backscattering. These predictions are given in Figure 8 for all three backscattering models with both measured and modelled soil moisture, and should be compared with the measured backscattering in Figure 1b. In this way, the procedure proposed by Lin (1994) and Wüthrich (1997) for calibrating the backscattering roughness parameters was tested. The measured correlation length was used as input as only one set of soil moisture data was available for calibration, and Jackson *et al*. (1997) suggests that RMS surface height is the most important roughness parameter for backscatter prediction. A summary of the RMS differences and r^2 values between the measured and retrieved RMS surface roughness parameter is given in Table IV. Here it can be seen that the r^2 value is greatest and both RMS and maximum difference in RMS surface roughness is least for the 1-cm model soil moisture. This is a reflection of the C-band SAR response to soil moisture in a soil layer of thickness closer to 1-cm than 15-cm.

A summary of the RMS errors and r^2 values between each of the predicted backscattering values and the ERS-2 observations is given in Table V for Julian day 265. When comparing with Table III, it may be seen that RMS errors were reduced for all three models (by up to 6·1 dB) and that r^2 values were increased slightly (by up to 0·1) for the IEM backscattering prediction, when the RMS surface roughness was calibrated. However, the r^2 values were still low (maximum of 0·17) for all situations, meaning that calibration has significantly improved the RMS error but not the correlation.

The comparison in Table V shows that there were comparable RMS errors in backscattering model predictions for all three backscattering models, and when measured soil moisture values were replaced with modelled soil moisture, when the RMS surface roughness had been calibrated. This would suggest that providing the backscattering model is calibrated to the site for which soil moisture measurements are required, through the roughness parameters, that predictions of backscattering are possible to within the calibration accuracy limits of the ERS-2 sensor (1 to 1·5 dB) using either of the three backscattering models used in this paper, providing the pixels are aggregated to a resolution of greater than 100 m $\times$ 100 m. This indicates that even with calibration of the backscattering model, measurement of soil moisture at the hillslope scale would not be possible using the ERS-2 SAR.

CONCLUSIONS

It was found that even when using the same input data there was a large variation in backscattering estimates from the three state-of-the-art backscattering models tested, with a RMS difference as large as 3·7 dB and r^2 as low as 0·53. Moreover, it was found that when using measurements of near-surface soil moisture and roughness from a 6 ha experimental catchment as input to these backscattering models, there were significant RMS errors (up to 8·4 dB) and negligible r^2 values (less than 0·1) when comparing the model output of backscattering with ERS-2 SAR observations. Spatial filtering of the ERS-2 SAR data had the effect of both increasing the r^2 (up to 0·25) and decreasing the RMS values (by up to 1·3 dB). Using model output of near-surface soil moisture (1 cm) in place of the measured near-surface soil moisture (15 cm) reduced the RMS errors slightly (by up to 2 dB) but did not improve the r^2 values. Using the first day of ERS-2 SAR observations and measured/model soil moisture to solve for the RMS surface roughness reduced the RMS

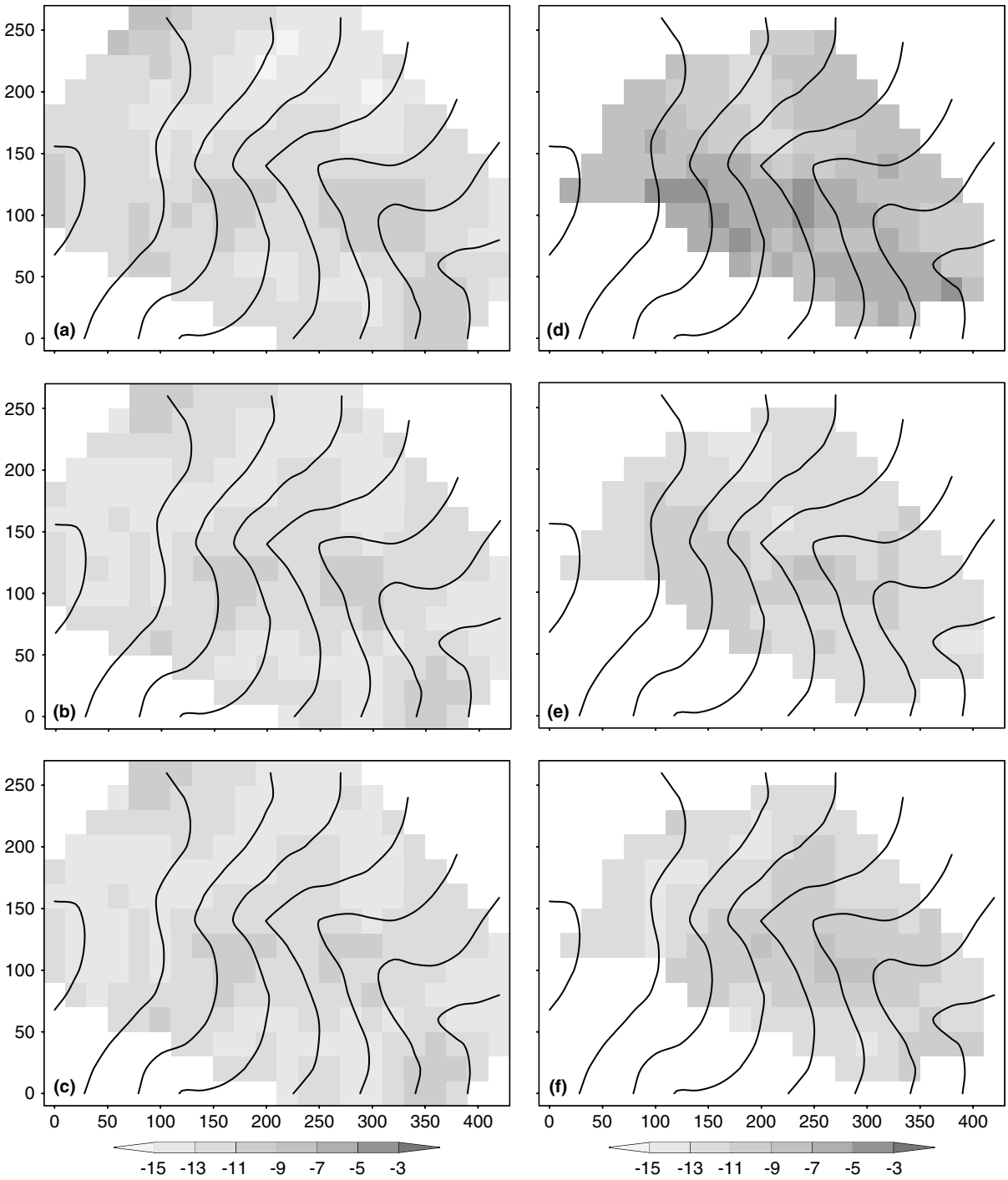

Figure 8. Predicted backscattering for Julian day 265 using inverted RMS surface roughness from Julian day 249 with: measured soil moisture and (a) IEM, (b) EM and (c) SEM backscattering models; modelled soil moisture and (d) IEM, (e) EM and (f) SEM backscattering models (dB). Contour lines are elevation with an interval of 5 m

errors for the second day to between 0·9 and 1·3 dB (when using a 3 × 3 filter) but made only marginal, if any, improvement to the r^2 values.

These results suggest that more work is required to improve the agreement between backscattering models. Furthermore, providing a site-specific surface roughness was calibrated then all models could satisfactorily predict the level of ERS-2 SAR backscatter, but not its spatial variation within a hillslope. Without calibration none of the models provided satisfactory predictions of backscatter level. Moreover, spatial filtering of 'speckle' in the ERS-2 data increased the r^2 values slightly, suggesting that ERS-2 backscatter data does not contain soil moisture information at less than the field scale. A similar conclusion was reached by Western *et al*. (submitted) in their study with AirSAR data. Thus, ERS-2 SAR backscatter data may provide field-scale soil moisture estimates but only with appropriate filtering and calibration of surface roughness parameters.

ACKNOWLEDGEMENTS

Support given by Anne Hsu in the georeferencing of ERS-2 scenes and Dinush Kurera in the analysis of those scenes is acknowledged. The authors are very grateful to Rudi Hoeben and Zhongbo Su for fruitful discussion and valuable comments.

REFERENCES

Altese E, Bolognani O, Mancini M, Troch PA. 1996. Retrieving soil moisture over bare soil from ERS-1 synthetic aperture radar data: sensitivity analysis based on a theoretical surface scattering model and field data. *Water Resources Research* **32**(3): 653–661.

Arya LM, Richter JC, Paris JF. 1983. Estimating profile water storage from surface zone soil moisture measurements under bare field conditions. *Water Resources Research* **19**(2): 403–412.

Autret M, Bernard R, Vidal-Madjar D. 1989. Theoretical study of the sensitivity of the microwave backscattering coefficient to the soil surface parameters. *International Journal of Remote Sensing* **10**(1): 171–179.

Beaudoin A, Le Toan T, Gwyn QHJ. 1990. SAR observations and modeling of the C-band backscatter variability due to multiscale geometry and soil moisture. *IEEE Transactions on Geoscience and Remote Sensing* **28**(5): 886–895.

Bindlish R, Barros AP. 2000. Multifrequency soil moisture inversion from SAR measurements with the use of IEM. *Remote Sensing of the Environment* **71**(1): 67–88.

Bolognani O, Mancini M, Rosso R. 1996. Soil moisture profiles from multifrequency radar data at basin scale. *Meccanica* **31**(1): 59–72.

Brown RJ, Manore MJ, Poirer S. 1992. Correlations between X-, C- and L-band imagery within an agricultural environment. *International Journal of Remote Sensing* **13**(9): 1645–1661.

Bruckler L, Witono H, Stengel P. 1988. Near surface soil moisture estimation from microwave measurements. *Remote Sensing of Environment* **26**: 101–121.

Chen KS, Yen SK, Huang WP. 1995. A Simple model for retrieving bare soil moisture from radar-scattering coefficients. *Remote Sensing of the Environment* **54**: 121–126.

Dobson MC, Ulaby FT. 1986. Active microwave soil moisture research. *IEEE Transactions on Geoscience and Remote Sensing* **GE-24**(1): 23–36.

Dubois PC, van Zyl J. 1994. An empirical soil moisture estimation algorithm using imaging radar. In *Proceedings, International Geoscience and Remote Sensing Symposium (IGARSS)*, Pasadena; 1573–1575.

Dubois PC, van Zyl J, Engman T. 1995. Measuring soil moisture with imaging radars. *IEEE Transactions on Geoscience and Remote Sensing* **33**(4): 915–926.

D' Urso G, Giacomelli A, Mancini M, Troch PA. 1994. The SESAR'93 experience on soil dielectric behaviour from ERS-1 satellite. In *Proceedings of the First Workshop on Data Collection and Data Analysis Issues for Spatial and Temporal Soil Moisture Mapping from ERS-1 and JERS-1 SAR Data and Macroscale Hydrologic Modelling (EV5V-CT94-0446),* De Troch FP, Su Z, Troch PA (eds). Institute for Agricultural Hydraulics, University of Naples; 1–13.

Engman ET. 1991. Application of microwave remote sensing of soil moisture for water resources and agriculture. *Remote Sensing of the Environment* **35**: 213–226.

Engman ET, Chauhan N. 1995. Status of microwave soil moisture measurements with remote sensing. *Remote Sensing of the Environment* **51**(1): 189–198.

Fung AK. 1994. *Microwave Scattering and Emission Models and their Applications*. Artech House: London; 573 pp.

Fung AK, Li Z, Chen KS. 1992. Backscattering from a randomly rough dielectric surface. *IEEE Transactions on Geoscience and Remote Sensing* **30**(2): 356–369.

Giacomelli A, Bacchiega U, Troch PA, Mancini M. 1995. Evaluation of surface soil moisture distribution by means of SAR remote sensing techniques and conceptual hydrological modelling. *Journal of Hydrolog* **166**: 445–459.

Hoeben R, Troch PA, Su Z, Mancini M, Chen K. 1997. Sensitivity of radar backscattering to soil surface parameters: a comparison between theoretical analysis and experimental evidence. In *Proceedings, International Geoscience and Remote Sensing Symposium (IGARSS),* Singapore; 1368–1370.

Hsieh CY, Fung AK. 1997. Application of an extended IEM to multiple surface scattering and backscatter enhancement. In *Proceedings, International Geoscience and Remote Sensing Symposium (IGARSS),* Singapore; 702–704.
Jackson TJ, Schmugge TJ. 1989. Passive microwave remote sensing system for soil moisture: some supporting research. *IEEE Transactions on Geoscience and Remote Sensing* **27**: 225–235.
Jackson TJ, Schmugge TJ, Engman ET. 1996. Remote sensing applications to hydrology : Soil moisture. *Hydrological Sciences Journal* **41**(4): 517–530.
Jackson TJ, McNairn H, Weltz MA, Brisco B, Brown R. 1997. First order surface roughness correction of active microwave observations for estimating soil moisture. *IEEE Transactions on Geoscience and Remote Sensing* **35**(4): 1065–1069.
Laur H, Bally P, Meadows P, Sanchez J, Schaettler B, Lopinto E, Esteban D. 1998. *ERS SAR Calibration: Derivation of the Backscattering Coefficient σ° in ESA ERS SAR PRI Products*. Document No. ES-TN-RS-PM-HL09, Issue 2, Rev. 5b, European Space Agency; 47.
Lin DS. 1994. On the suitability of field surface roughness measurements as input to microwave backscattering models. In *Proceedings of the First Workshop on Data Collection and Data Analysis Issues for Spatial and Temporal Soil Moisture Mapping from ERS-1 and JERS-1 SAR Data and Macroscale Hydrologic Modeling (EV5V-CT94-0446)*, De Troch FP, Su Z, Troch PA (eds). Institute for Agricultural Hydraulics, University of Naples; 91–98.
Lin DS, Wood EF, Beven K, Saatchi S. 1994. Soil moisture estimation over grass-covered areas using AIRSAR. *International Journal of Remote Sensing* **15**(11): 2323–2343.
Moran MS, Hymer DC, Qi J, Sano EE. 2000. Soil moisture evaluation using multi-temporal synthetic aperture radar (SAR) in semiarid rangeland. *Agricultural and Forest Meteorology* **105**(1–3): 69–80.
Newton RW, Black QR, Makanvand S, Blanchard AJ, Jean BR. 1982. Soil moisture information and thermal microwave emission. *IEEE Transactions on Geoscience and Remote Sensing* **GE-20**(3): 275–281.
Newton RW, Heilman JL, van Bavel CHM. 1983. Integrating passive microwave measurements with a soil moisture/heat flow model. *Agricultural Water Management* **7**: 379–389.
Njoku EG, Entekhabi D. 1996. Passive microwave remote sensing of soil moisture. *Journal of Hydrology* **184**: 101–129.
Oh Y, Sarabandi K, Ulaby FT. 1992. An empirical model and an inversion technique for radar scattering from bare soil surfaces. *IEEE Transactions on Geoscience and Remote Sensing* **30**(2): 370–381.
Oh Y, Sarabandi K, Ulaby FT. 1994. An inversion algorithm for retrieving soil moisture and surface roughness from polarimetric radar observation. In *Proceedings, International Geoscience and Remote Sensing Symposium (IGARSS),* Pasadena; 1582–1584.
Peplinski NR, Ulaby FT, Dobson MC. 1995. Dielectric properties of soils in the 0·3–1·3 GHz range. *IEEE Transactions on Geoscience and Remote Sensing* **33**(3): 803–807.
Raju S, Chanzy A, Wigneron J, Calvert J, Kerr Y, Laguerre L. 1995. Soil moisture and temperature profile effects on microwave emission at low frequencies. *Remote Sensing of the Environment* **54**: 85–97.
Robinson N. 1966. *Solar Radiation*. Elsevier: Amsterdam; 347 pp.
Roth K, Schulin R, Flühler H, Attinger W. 1990. Calibration of time domain reflectometry for water content measurement using a composite dielectric approach. *Water Resources Research* **26**(10): 2267–2273.
Sano EE, Huete AR, Troufleau D, Moran MS, Vidal A. 1998. Relation between ERS-1 synthetic aperture radar data and measurements of surface roughness and moisture content of rocky soils in a semiarid rangeland. *Water Resources Research* **34**(6): 1491–1498.
Schmugge T. 1985. Remote sensing of soil moisture. In *Hydrological Forecasting*, Anderson MG, Burt TP (eds). Wiley: Chichester; 101–124.
Schmugge TJ, Choudhury BJ. 1981. A comparison of radiative transfer models for predicting the microwave emission from soils. *Radio Science* **16**(5): 927–938.
Schmulluis C, Furrer R. 1992. Frequency dependence of radar backscattering under different moisture conditions of vegetation-covered soils. *International Journal of Remote Sensing* **13**(12): 2233–2245.
Shi J, Wang J, Hsu A, O'Neill P, Engman ET. 1997. Estimation of bare surface soil moisture and surface roughness parameter using L-band SAR image data. *IEEE Transactions on Geoscience and Remote Sensing* **35**(5): 1254–1266.
Su Z, Troch PA, de Troch FP. 1997. Remote sensing of bare soil moisture using EMAC/ESAR data. *International Journal of Remote Sensing* **18**(10): 2105–2124.
Troch PA, de Troch FP, Debruyckere L, Cosyn B. 1994. Organization of the summer '94 Field Campaigns in the Zwalm Test Site. In *Proceedings of the First Workshop on Data Collection and Data Analysis Issues for Spatial and Temporal Soil Moisture Mapping from ERS-1 and JERS-1 SAR Data and Macroscale Hydrologic Modelling (EV5V-CT94-0446)*, de Troch FP, Su Z, Troch PA (eds). Institute for Agricultural Hydraulics, University of Naples; 14–24.
Ulaby FT, Batliva PP. 1976. Optimum radar parameters for mapping soil moisture. *IEEE Transactions on Geoscience and Electronics* **GE-14**(2): 81–93.
Ulaby FT, Batliva PP, Dobson MC. 1978. Microwave backscatter dependence on surface roughness, soil moisture and soil texture; Part 1—bare soil. *IEEE Transactions on Geoscience and Electronics* **GE-16**(4): 286–295.
Ulaby FT, Moore RK, Fung AK. 1986. *Microwave Remote Sensing, Active and Passive; Volume III: from Theory to Applications*. Artech House: Norwood, MA; 1097 pp.
Ulaby FT, Dubois PC, van Zyl J. 1996. Radar mapping of surface soil moisture. *Journal of Hydrology* **184**: 57–84.
van de Griend AA, Engman ET. 1985. Partial area hydrology and remote sensing. *Journal of Hydrology* **81**: 211–251.
Van Oevelen PJ. 1998. Soil moisture variability: a comparison between detailed field measurements and remote sensing measurement techniques. *Hydrological Sciences Journal* **43**(4): 511–520.
Van Zyl JJ. 1993. The effects of topography on the radar scattering from vegetated areas. *IEEE Transactions on Geoscience and Remote Sensing* **31**(1): 153–160.
Verhoest NEC, Troch PA, Paniconi C, de Troch FP. 1998. Mapping basin scale variable source areas from multitemporal remotely sensed observations of soil moisture behaviour. *Water Resources Research* **34**(12): 3235–3244.

Walker JP, Troch PA, Mansini M, Willgoose GR, Kalma JD. 1997. Profile soil moisture estimation using the modified IEM. In *Proceedings, International Geoscience and Remote Sensing Symposium (IGARSS)*, Stein T. (ed). Singapore 3—8 August, 1263–1265.

Walker JP, Willgoose GR, Kalma JD. 2001. The nerrigundah data set: soil moisture patterns, soil characteristics and hydrological flux measurements. *Water Resources Research* **37**(11): 2653–2658.

Walker JP, Willgoose GR, Kalma JD. 2002. Three-dimensional soil moisture profile retrieval by assimilation of near-surface measurements: simplified Kalman filter covariance forecasting and field application. *Water Resources Research* **38**(12): 1301. DOI:10·1029/2002WR001545.

Wang JR, Engman ET, Mo T, Schmugge TJ, Shiue JC. 1987. The effects of soil moisture, surface roughness, and vegetation on L-Band emissions and backscatter. *IEEE Transactions on Geoscience and Remote Sensing* **GE-25**(6): 825–833.

Wegmüller U, Mätzler C, Hüppi R, Schanda E. 1994. Active and passive microwave signature catalogue on bare soil (2–12 GHz). *IEEE Transactions on Geoscience and Remote Sensing* **32**(3): 698–702.

Western A, Grayson R, Blöschl G, Willgoose G, McMahon T. 1997. The Tarrawarra Project: high resolution spatial measurement and analysis of hydrological response. In *Proceedings, MODSIM 97 International Congress on Modelling and Simulation,* McDonald AD, McAleer M (eds). Hobart; 403–408.

Western AW, Grayson RB, Sadek T, Turral H. Measuring soil moisture patterns with AirSAR at Tarrawarra. *Remote Sensing of the Environment* (submitted to Journal of Hydrology).

Wilheit TT. 1978. Radiative transfer in a plane stratified dielectric. *IEEE Transactions on Geoscience and Electronics* **GE-16**(2): 138–143.

Wüthrich M. 1997. *In-situ measurement and remote sensing of soil moisture using time domain reflectometry, thermal infrared and active microwaves*. PhD thesis, Naturwissenschaftlichen Fakultät der Universität Basel.

Zegelin S. 1996. Soil moisture measurement. In *Field Measurement Techniques in Hydrology—Workshop Notes*, Cooperative Research Centre for Catchment Hydrology, Corpus Christi College, Clayton; C1–C22.

